ORIGINAL ARTICLE

Tree growth and climate in the Pacific Northwest, North America: a broad-scale analysis of changing growth environments

Whitney L. Albright[1]* and David L. Peterson[2]

[1]University of Washington, School of Environmental and Forest Sciences, Seattle, WA, 98195, USA, [2]US Forest Service Pacific Northwest Research Station, Seattle, WA, 98195, USA

ABSTRACT

Aim Climate change in the 21st century will affect tree growth in the Pacific Northwest region of North America, although complex climate–growth relationships make it difficult to identify how radial growth will respond across different species distributions. We used a novel method to examine potential growth responses to climate change at a broad geographical scale with a focus on visual inspection of patterns and applications beyond sampled areas.

Location Washington and Oregon, USA.

Methods We examined projected changes in climate within species distributions of mountain hemlock (*Tsuga mertensiana*), subalpine fir (*Abies lasiocarpa*), Douglas-fir (*Pseudotsuga menziesii*) and ponderosa pine (*Pinus ponderosa*) in Washington and Oregon based on three different future climate scenarios. By drawing on knowledge from previous climate–growth studies and organizing information into climate space plots, we inferred directional changes in future radial growth.

Results Increased moisture stress will reduce growth throughout the distribution of Douglas-fir, but growth may increase at some energy-limited locations. Decreased snowpack will increase growing season length and increase growth of subalpine fir and mountain hemlock at most locations, although growth may decrease at some low-elevation sites.

Main conclusions An altered Pacific Northwest climate will elicit different growth responses from common conifer species within their current distributions. The methodology developed in this study allowed us to qualitatively extrapolate climate–growth relationships from individual sites to entire species distributions and can identify growth responses where climate–growth data are limited.

*Correspondence: Whitney Albright, California Department of Fish and Wildlife, 1416 9th Street, Sacramento, CA 95814, USA.
E-mail: Whitney.Albright@wildlife.ca.gov

INTRODUCTION

Previous studies have documented relationships between climatic variability and radial growth of tree species in the Pacific Northwest region of North America (PNW), typically calculating correlations between climate variables and ring-width series (Fritts, 1976; Chen *et al.*, 2010; Huang *et al.*, 2010). Climate–growth relationships in the PNW have been examined for four species in the family Pinaceae: mountain hemlock, *Tsuga mertensiana* (Bong.) Carrière (Gedalof &

Smith, 2001; Peterson & Peterson, 2001); subalpine fir, *Abies lasiocarpa* (Hooker) Nuttall (Peterson & Peterson, 1994; Peterson *et al.*, 2002); Douglas-fir, *Pseudotsuga menziesii* (Mirb.) Franco (Case & Peterson, 2005; Littell *et al.*, 2008); and ponderosa pine, *Pinus ponderosa* Douglas ex. C. Lawson (Kusnierczyk & Ettl, 2002). Predictions of the effects of climate change on growth have been made based on climate–growth relationships (Laroque & Smith, 2003).

Growth variability is best explained by climate variables that express prevailing environmental constraints, or limiting

factors. If the factors most strongly limiting growth are related to available energy (e.g. temperature, growing season length), growth environment can be considered primarily energy-limited; whereas, if growth is limited by climatic factors affecting water availability and evaporative demand (e.g. solar radiation, evapotranspiration), growth environment can be considered primarily water-limited. Energy- and water-limitation are in fact relative terms with a continuum in between. Throughout their respective distributions, mountain hemlock and subalpine fir are predominantly energy-limited (Gedalof & Smith, 2001; Peterson & Peterson, 2001; Peterson et al., 2002), and Douglas-fir and ponderosa pine are predominantly water-limited (Kusnierczyk & Ettl, 2002; Case & Peterson, 2005; Littell et al., 2008). Across a species' distribution, water and energy both limit tree growth to some extent as a function of elevation, topography, microclimate and soils.

Climate accounts for only a portion of growth variability, but will change somewhat predictably in future decades (Randall et al., 2007). In order to examine the effects of climate change on a tree species, one would ideally have climate–growth data across its entire distribution. However, only limited climate–growth data from specific sites are generally available for extrapolating climate–growth relationships across the geographical domain of interest.

Mountain ecosystems contain a large amount of climatic variation over small geographical distances (Peterson et al., 1997; Fagre et al., 2003). The climatic gradient across the PNW is attributed to several atmospheric drivers and topographic features. The Cascade Range is a barrier between coastal maritime climate (wet winter, dry summer) and interior continental climate (dry year-round, high temperature fluctuations). Orographic precipitation and rain shadows caused by the Cascades and Olympic Mountains are dominant features; annual precipitation varies from > 500 cm in the western Olympics, to < 50 cm in the eastern Olympics (Henderson et al., 1989), to < 20 cm east of the Cascades (Franklin & Dyrness, 1988). Sea-level pressure and sea-surface temperature fluctuations in the Pacific Ocean (e.g. Pacific Decadal Oscillation, El Niño–Southern Oscillation) are important sources of climatic variability (Mantua et al., 1997).

Climate–growth variability as a function of heterogeneity of topography and climate has been documented across the PNW (Peterson & Peterson, 2001; Case & Peterson, 2005; Holman & Peterson, 2006; Nakawatase & Peterson, 2006; Littell et al., 2008). Because tree growth is not spatially uniform, one must consider the range of climate experienced by a species (or 'climate space') to understand growth response (Littell et al., 2008). Variables such as climatic water deficit and snow-water equivalent assess interactions between water balance and energy balance from a plant perspective (Stephenson, 1990, 1998; Lookingbill & Urban, 2005; Shinker & Bartlein, 2010). Recent availability of spatially explicit projections of these variables allows them to be integrated in climate space, capturing meaningful effects of changing climate.

In the PNW, climate change is projected to increase winter and summer temperatures and decrease snowpack and summer precipitation (Miles et al., 2010). Annual average temperature[1] in the PNW is expected to increase 1.1 °C by the 2020s, 1.8 °C by the 2040s, and 3.0 °C by the 2080s (Mote & Salathé, 2010). Because tree growth is limited by climate and sensitive to climatic variability, altered tree growth across the PNW is almost certain.

In this study, we identified changes in growth environments of mountain hemlock, subalpine fir, Douglas-fir and ponderosa pine, using projected changes in climate variables. Growth environments were defined by actual evapotranspiration (AET), climatic water deficit (DEF) and snow-water equivalent (SWE). We examined changes in these variables under different warming scenarios to assess how growth environments will change during the 21st century. By plotting each species distribution in climate space, we inferred growth responses to projected climate changes based on climate–growth relationships. By assessing future growth trends, we will better understand where potential growth increases and decreases may occur and which species will be resilient in a warmer climate.

MATERIALS AND METHODS

Part 1: Species distributions in climate space

We used bivariate plots of climate variables to visualize current and future climate space of each species distribution in Washington and Oregon (Figs 1 & 2). The following sections describe climatic data sets and species distribution maps, how climate space plots were developed, and how changes in growth environments were assessed.

Climatic data

Historical and projected climatic data used to create climate space graphs were generated by the Variable Infiltration Capacity (VIC) hydrological model (Liang et al., 1994; Nijssen et al., 1997; Elsner et al., 2010). VIC is driven by output from statistically downscaled global climate models (GCMs) and historical observations to provide daily and monthly estimates to 1/16th degree (c. 6 km × 7 km). Vegetation and soil parameters are input to the VIC model, with emphasis on calculating evapotranspiration, soil moisture and SWE. The model is intended for application to areas > 10,000 km², which fits our study (Elsner et al., 2010). We obtained VIC climate projections from 10 GCMs, each paired with Intergovernmental Panel on Climate Change (IPCC) emission scenarios A1B and B1 (Nakićenović & Swart, 2000). GCM output was downscaled using the hybrid-delta method (Hamlet et al., 2010), and projections were developed for 30-year time periods centred on the 2020s

---

[1]Annual average temperature is based on a weighted average of model simulations by 20 global climate models and two IPCC emissions scenarios, A1B and B1.
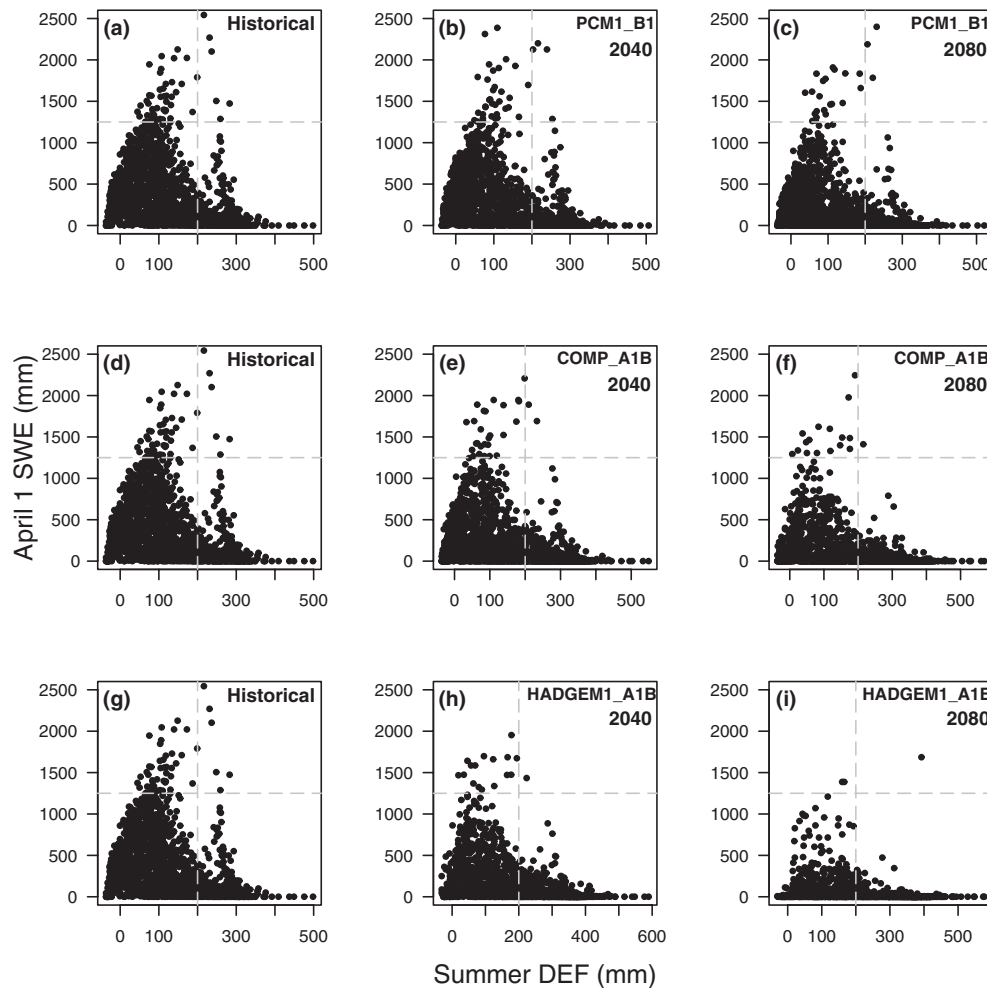
Figure 1 Climate space plots for subalpine fir (*Abies lasiocarpa*) in the Pacific Northwest states of Oregon and Washington using summer climatic water deficit (DEF) and April 1 snow-water equivalent (SWE). Panels (b) and (c) in the first row represent climate projections from the PCM1_B1 model (low-end warming scenario). Panels (e) and (f) in the second row represent climate projections from the COMP_A1B model (medium warming scenario), and panels (h) and (i) in the third row represent climate projections from the HADGEM1_A1B model (high-end warming scenario). Plots in the first column are identical and represent climate data from the historical time period. Plots in the second and third columns represent data from the 2040s and 2080s, respectively. The plots exclude a small number of sites with extremely high SWE in order to focus on the majority of the species distribution. Lines are placed at the same location on each plot to provide a frame of reference.

(2010–2039), 2040s (2030–2059), and 2080s (2070–2099) (Climate Impacts Group, 2010).

We used a subset of climate projections, based on three GCMs and two emission scenarios, to capture a range of future growth environments. HADGEM1_A1B is the warmest scenario in the PNW throughout the 21st century, and PCM1_B1 is among the coolest (Mote & Salathé, 2010). COMP_A1B represents a medium warming scenario that averages out model biases of the 10 GCMs and closely matches observations.

Projections of increased annual average temperature in the PNW (between 124–111° W and 41.5–49.5° N) differ between A1B and B1 scenarios by 0.1 °C in the 2020s, 0.6 °C in the 2040s, and 1.5 °C in the 2080s (Mote & Salathé, 2010). Climatic data were examined from HADGEM1_A1B, COMP_A1B and PCM1_B1 for the 2040s and 2080s.

Climate variables include AET, DEF and April 1 SWE. DEF represents evaporative demand that cannot be met by available water at a given site, calculated as potential evapotranspiration (PET) minus AET (Stephenson, 1990); AET measures actual availability of water that could be evaporated from a site. PET is the expected amount of evaporative water loss given unlimited water supply, depending on heat, radiation and wind (Stephenson, 1990). Of the PET calculations in VIC, we used one based on natural vegetation surface and aerodynamic resistance from a tree canopy.

Climate space plots

In order to utilize VIC data for a given species, VIC output was spatially confined by species geographical distributions. The VIC output grid was overlain on species distribution
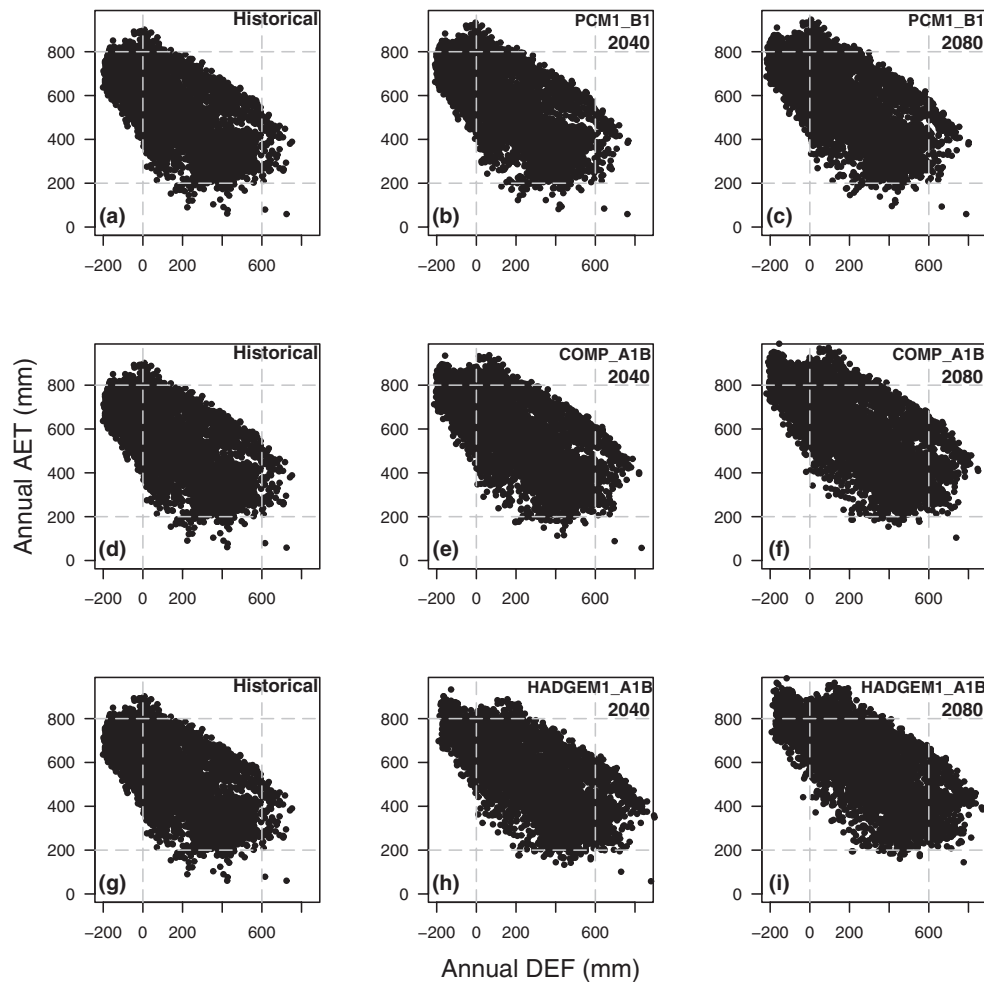
Figure 2 Climate space plots for Douglas-fir (*Pseudotsuga menziesii*) in the Pacific Northwest states of Oregon and Washington using annual climatic water deficit (DEF) and annual actual evapotranspiration (AET). Panels (b) and (c) in the first row represent climate projections from the PCM1_B1 model (low-end warming scenario). Panels (e) and (f) in the second row represent climate projections from the COMP_A1B model (medium warming scenario), and panels (h) and (i) in the third row represent climate projections from the HADGEM1_A1B model (high-end warming scenario). Plots in the first column are identical and represent climate data from the historical time period. Plots in the second and third columns represent data from the 2040s and 2080s, respectively. Lines are placed at the same location on each plot to provide a frame of reference.

maps (Little, 1971), and VIC grid cells falling within the distribution were identified. Climate space plots were created wherein each point was the climate variable value in a VIC cell within each species distribution. Two bivariate plots were drawn: annual DEF versus annual AET, and summer DEF versus April 1 SWE. April 1 SWE is a direct output of VIC. Annual PET and AET were calculated from VIC output as the sum of monthly values; annual DEF was calculated as annual PET minus annual AET. Summer DEF was calculated as the sum of June/July/August PET minus the sum of June/July/August AET. Each variable was averaged over a 1970–1999 reference period, then recalculated for 2030–2059 and 2070–2099. All calculations and graphs were produced in R 2.9.2 (R Development Core Team, 2009). Historical and projected climatic conditions are presented in Figs 1 & 2 and Table 1.

Comparing historical and projected climatic conditions across species distributions

We calculated summary statistics to assess the magnitude and direction of differences between historical and projected climatic conditions across each species distribution. Summary statistics included median value of each climate variable for the historical reference period and each climate model projection for the end of the century. We then used the Wilcoxon signed rank test for paired data to determine if there was a significant shift between historical and projected climate for each variable and species. Although the nonparametric Wilcoxon test has lower statistical power than a *t*-test, it was used because most variable projections deviate from normality (based on quantile–quantile plots).

Table 1 Projected changes, based on three global climate model projections and two emission scenarios, in April 1 snow-water equivalent (SWE), summer climatic water deficit (DEF), annual climatic water deficit (DEF), and annual actual evapotranspiration (AET) by the 2080s relative to the historical reference period for subalpine fir (*Abies lasiocarpa*), mountain hemlock (*Tsuga mertensiana*), Douglas-fir (*Pseudotsuga menziesii*) and ponderosa pine (*Pinus ponderosa*) in the Pacific Northwest states of Oregon and Washington. Values represent relative changes in median climate variable values across a species distribution. Negative values indicate decreases relative to the historical reference period, and positive values represent increases. Wilcoxon signed rank test for all variables and scenarios produced *P*-values < 0.001.

Species variable	Climate model		
	PCM1_ B1	COMP_ A1B	HADGEM1_ A1B
Subalpine fir			
Δ Median SWE (mm)	−204	−229	−232
Δ Median summer DEF (mm)	11	71	113
Δ Median annual DEF (mm)	26	102	142
Δ Median annual AET (mm)	27	43	61
Mountain hemlock			
Δ Median SWE (mm)	−306	−346	−348
Δ Median summer DEF (mm)	−11	28	77
Δ Median annual DEF (mm)	8	63	102
Δ Median annual AET (mm)	44	71	89
Douglas-fir			
Δ Median SWE (mm)	0	0	0
Δ Median summer DEF (mm)	−17	82	120
Δ Median annual DEF (mm)	24	101	129
Δ Median annual AET (mm)	30	47	59
Ponderosa pine			
Δ Median SWE (mm)	−2	−2	−2
Δ Median summer DEF (mm)	25	79	106
Δ Median annual DEF (mm)	38	104	131
Δ Median annual AET (mm)	11	23	26

Part 2: Assessing spatial variation in growth responses

Sampling sites from previous climate–growth studies in which climate–growth relationships had already been identified were highlighted in climate space for each species (Figs 3–5). Cells were grouped by geographical location, labelled as water- or energy-limited, and tracked through time to illustrate trajectories of each cell in climate space through the end of the century. Climate variable values were examined at selected cells to illustrate differences among cells along elevation and east–west/north–south sampling transects (Tables 2–4). The climate of individual cells provides insight into local responses to growth environments, and cells grouped by geographical location provide insight into trends of species responses across climatic gradients. Inferences regarding growth responses to climate change were drawn from visual assessment of patterns and changes in climate space plots and supplemental information.

Study selection and sampling site location

Climate–growth information was extracted from published analyses of tree species in Washington and Oregon. Sampling locations were recorded, and when available, field notes with site descriptions and topographic layers were used in ArcGIS 9.3 (ESRI, Redlands, CA) to pinpoint sampling sites (see Appendix S1 in Supporting Information). All locations were converted to 1/16th degree and located on the VIC grid. The corresponding VIC cell containing each location was highlighted in climate space. Multiple sampling sites often fell within a single VIC cell. Distribution of species and sampled VIC cells are shown in Fig. 6.

Climate–growth data

Each of the studies from which sampling sites were obtained reported a climate–growth related chronology for each site. These relationships were used to determine the climate factor predominantly limiting growth at each site and corresponding sampled cell. Most studies performed similar steps to identify climate–growth relationships. Tree cores were extracted and measured for each sample tree, a growth time series (site chronology) was developed for each site, and descriptive statistics were calculated for each chronology (Fritts, 1976; Cook & Kairiukstis, 1990). Nakawatase & Peterson (2006) converted ring-width measurements to annual diameter increments and then to basal area increments (BAI); individual BAI time series were standardized to create mean growth time series.

  Some studies used factor analysis to describe common patterns among site chronologies (Peterson & Peterson, 1994, 2001; Peterson *et al.*, 2002; Case & Peterson, 2005; Nakawatase & Peterson, 2006). We used the factor chronology with the highest correlation, and the climate variable with the highest correlation with that factor chronology to define the climate–growth relationship. Some studies used response function analysis to relate site chronologies to individual climate variables (Gedalof & Smith, 2001; Kusnierczyk & Ettl, 2002; Littell *et al.*, 2008). We used the climate variable with the highest correlation with growth to represent the climate–growth relationship. Correlations for each site are summarized in Appendix S1.

Determining water- or energy-limitation from climate–growth data

The dominant climate variable affecting growth for each site and the relationship of the variable with growth (positive or negative), were used to characterize each site as water- or energy-limited. A categorical approach to classifying each cell was applied. In an environment where energy is limiting, growth is typically negatively correlated with winter precipitation and positively correlated with summer and winter temperature (Ettl & Peterson, 1995; Peterson, 1998). Cells with these climate–growth relationships were considered
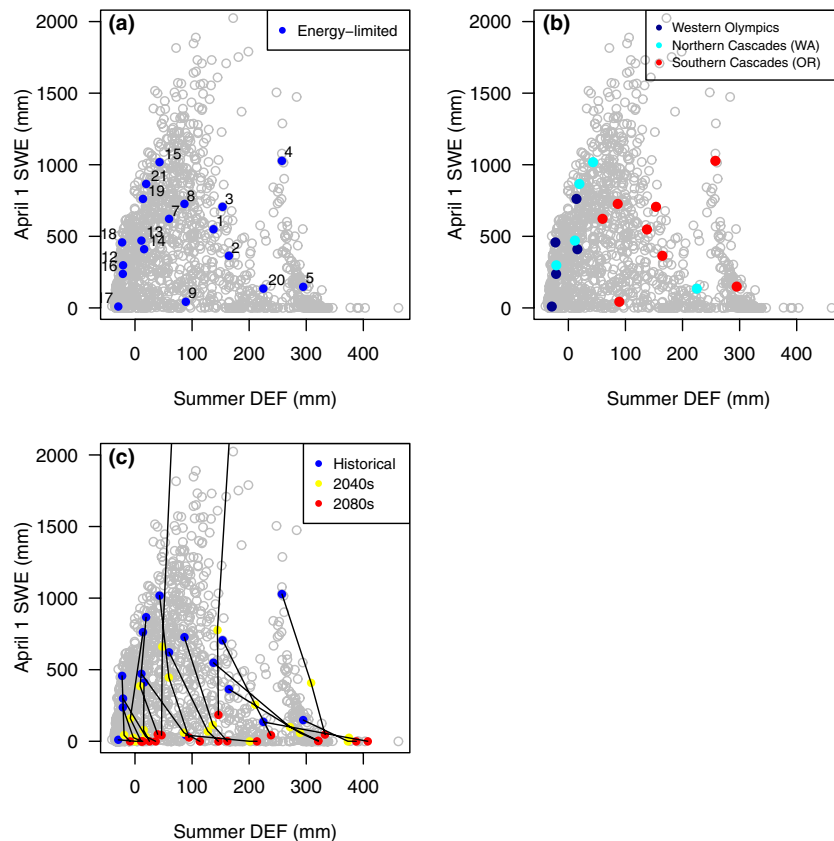
Figure 3 Mountain hemlock (*Tsuga mertensiana*) distribution in climate space in the Pacific Northwest states of Oregon and Washington [summer climatic water deficit (DEF) versus April 1 snow-water equivalent (SWE)] with sampled cells highlighted in panel (a) and cells grouped by geographical region in panel (b). Panel (c) illustrates the movement of individual cells in climate space from the historical time period to the 2040s and 2080s as projected by the HADGEM1_A1B (high-end warming) scenario. Lines connect the historical point of each cell to its projected position in climate space in the 2040s and 2080s. The graph excludes a small number of sites with extremely high SWE in order to focus on the majority of the species distribution.

energy-limited. In an environment where water is limiting, species growth is typically positively correlated with summer and winter precipitation and negatively correlated with summer temperature (Knutson & Pyke, 2008; Littell *et al.*, 2008). Cells with these climate–growth relationships were considered water-limited. Sampled VIC cells were labelled in climate space based on the majority of cases within a cell. If there was an equal amount of water- and energy-limited sites, the limitation was based on the highest climate–growth correlation among sites. See Appendix S1 for water- and energy-limited designations for each site.

RESULTS

Part 1: Climate space graphs

Subalpine fir and mountain hemlock distributions will experience much lower snow-water equivalent (SWE) in future decades relative to the historical reference period (climate space plots created for mountain hemlock and subalpine fir are similar, so only plots for subalpine fir are presented; Fig. 1). Projected decreases are highest for HADGEM1_A1B,

followed by COMP_A1B and PCM1_B1. The downward shift of points in the climate space plots, demonstrating SWE decrease, suggests that VIC cells with a higher initial SWE are most sensitive to change. It was difficult to discern projected changes in summer climatic-water deficit (DEF) by visual inspection, but average DEF change across a species' distribution suggests that as SWE decreases, DEF will increase (Table 1). SWE decreases will be larger for mountain hemlock, and summer DEF increases will be larger for subalpine fir.

Within Douglas-fir and ponderosa pine distributions, annual DEF and actual evapotranspiration (AET) in climate space best capture the moisture stress that limits growth. Increased annual DEF is projected throughout the 21st century, especially for the HADGEM1_A1B scenario (Fig. 2). Visual shifts in AET were difficult to detect, because AET increases only slightly by the end of the century in both species distributions (Table 1). Increases in DEF not accompanied by comparable increases in AET suggest a likely augmentation of moisture stress. Increases in annual DEF are slightly higher for ponderosa pine, and increases in annual AET are slightly higher for Douglas-fir. Annual DEF values cannot in
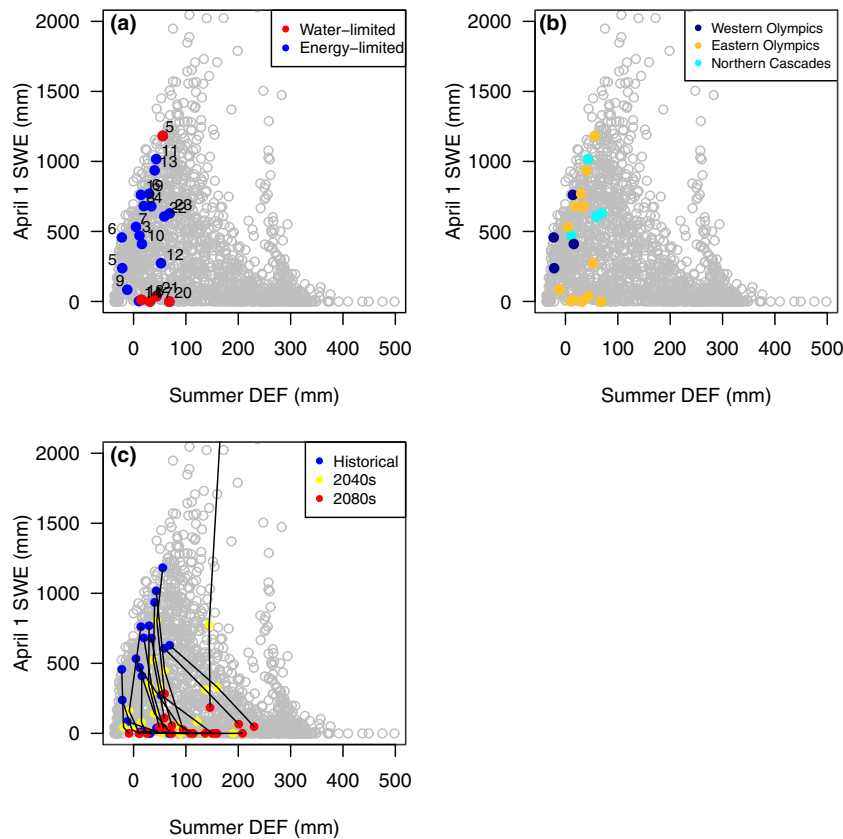
Figure 4 Subalpine fir (*Abies lasiocarpa*) distribution in climate space in the Pacific Northwest states of Oregon and Washington [summer climatic water deficit (DEF) versus April 1 snow-water equivalent (SWE)] with sampled cells highlighted in panel (a), and cells grouped by geographical region in panel (b). Panel (c) illustrates the movement of individual cells in climate space from the historical time period to the 2040s and 2080s as projected by the HADGEM1_A1B (high-end warming) scenario. Lines connect the historical point of each cell to its projected position in climate space in the 2040s and 2080s. The graph excludes a small number of sites with extremely high SWE in order to focus on the majority of the species distribution.

reality be negative as shown on the graph, but are assumed to be close to zero; calculation of negative DEF values is a limitation of the VIC model that is currently being resolved. The projected changes described above are statistically significant (all *P*-values < 0.001).

## Part 2: Spatial variation in growth responses

Figures 3–5 each display one graph in which sampled VIC cells are labelled according to their limitation status (water or energy) (panel a), a second graph in which VIC cells are colour-coded based on geographical location (panel b), and a third graph that illustrates the trajectory of each cell in climate space through time according to the HAD-GEM1_A1B scenario (panel c). These panels provide insight into how conditions in sampled cells, and perhaps unsampled cells in the same area of climate space, are changing.

Tree species were sampled across much of their respective distributions in climate space, with the exception of ponderosa pine, for which we did not analyse spatial variation in growth. Due to its limited representation in climate space,

we have less confidence in our ability to make inferences about changes in future growth.

Subalpine fir and mountain hemlock display similar geographical patterns in values and projected changes in DEF and SWE. Sampled cells within both species distributions display increasing DEF along west–east and north–south gradients (Figs 3b & 4b). Southernmost sites generally had among the highest historical DEF values of all sites for both species. Western and northernmost subalpine fir and mountain hemlock sites experience large decreases in SWE by the 2040s (Figs 3c & 4c). Many southern Cascade cells are also projected to have decreased SWE and will simultaneously have increased DEF; this includes cells that contain sites for drier mountain hemlock habitats. Water-limited subalpine fir cells in the eastern Olympics also follow the trajectory of lower SWE, moving towards increasing DEF on the *x*-axis along the lower limit of the graph (Fig. 4a,c).

For Douglas-fir, east–west gradients are evident, with lower AET and higher DEF from the western Olympics to the Cascades (Fig. 5b). Although Douglas-fir was not sampled in the southern Cascades, graphs of annual DEF versus latitude (not shown) displayed an increase in annual DEF
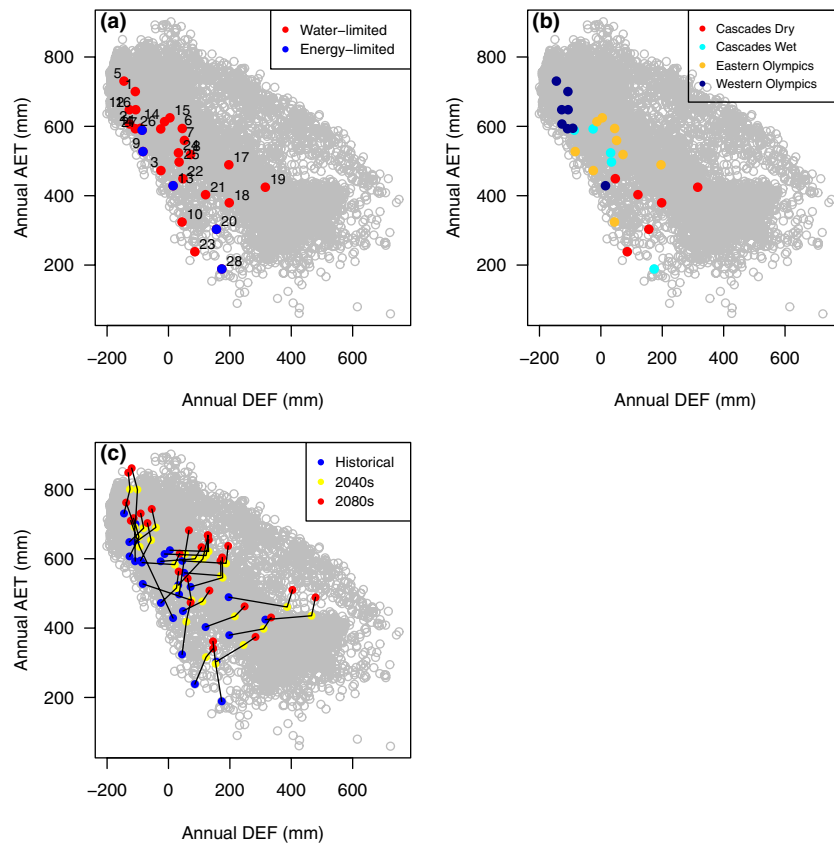
Figure 5 Douglas-fir (*Pseudotsuga menziesii*) distribution in climate space in the Pacific Northwest states of Oregon and Washington [annual climatic water deficit (DEF) versus annual actual evapotranspiration (AET)] with sampled cells highlighted in panel (a), and cells grouped by geographical region in panel (b). Panel (c) illustrates the movement of individual cells in climate space from the historical time period to the 2040s and 2080s as projected by the HADGEM1_A1B (high-end warming) scenario. Lines connect the historical point of each cell to its projected position in climate space in the 2040s and 2080s.

Table 2 Projected changes, based on three global climate model projections and two emission scenarios, in April 1 snow-water equivalent (SWE) and summer climatic water deficit (DEF) by the 2080s relative to the historical reference period. Values represent relative changes in climate variable values in selected mountain hemlock (*Tsuga mertensiana*)-sampled cells in the Pacific Northwest states of Oregon and Washington. General cell locations and site elevations are provided along with historical and projected values for climate variables. Cells correspond to cells 8, 9, 18 and 20, respectively, in Fig. 3. See Appendix S1 for additional site information. Negative values indicate decreases relative to the historical reference period, and positive values represent increases. These sites were selected because they represent elevation and geographical ranges of the species' sampled distribution (i.e. low to high elevation sites and north–south, east–west gradients).

Cell	Site elevation(s)	Climate variable	Climate model		
			PCM1_B1	COMP_A1B	HADGEM1_A1B
Mt Hood, OR	1920 m	SWE (mm)	−509	−668	−726
		Summer DEF (mm)	−18	35	75
Mt Hood, OR	1585 m	SWE (mm)	−43	−43	−43
		Summer DEF (mm)	18	85	125
Hoh Lake, WA	1164–1315 m	SWE (mm)	−427	−457	−457
		Summer DEF (mm)	−10	−6	14
Mt Baker, WA	1330 m	SWE (mm)	−120	−125	−135
		Summer DEF (mm)	59	128	183

from the northern to southern edge of the species distribution (the upper-right 'wing' of Fig. 5 that appears unsampled contains mainly southern Cascade cells). Cells in the western

Olympics with historically high AET are projected to experience increased AET with only minor increases in DEF (Fig. 5c). Moving eastward, cell projections gradually show

Table 3 Projected changes, based on three global climate model projections and two emission scenarios, in April 1 snow-water equivalent (SWE) and summer climatic water deficit (DEF) by the 2080s relative to the historical reference period. Values represent relative changes in climate variable values in selected subalpine fir (*Abies lasiocarpa*)-sampled cells in the Pacific Northwest states of Oregon and Washington. General cell locations and site elevations are provided along with historical and projected values for climate variables. Cells correspond to cells 16, 20, 11 and 3, respectively, in Fig. 4. See Appendix S1 for additional site information. Negative values indicate decreases relative to the historical reference period, and positive values represent increases. These sites were selected because they represent elevation and geographical ranges of the species sampled distribution (i.e. low to high elevation sites and north–south, east–west gradients).

Cell	Site elevation(s)	Climate Variable	Climate model		
			PCM1_B1	COMP_A1B	HADGEM1_A1B
Hoh Watershed, WA	1164–1400 m	SWE (mm)	−427	−455	−457
		Summer DEF (mm)	−10	−6	14
Blue Mountain, WA	1340 m	SWE (mm)	0	0	0
		Summer DEF (mm)	21	88	140
Lake Minotaur, WA	1740 m	SWE (mm)	−514	−768	−991
		Summer DEF (mm)	−32	−5	51
Lake Minotaur, WA	1570 m, 1630 m	SWE (mm)	−425	−467	−471
		Summer DEF (mm)	12	52	102

Table 4 Projected changes, based on three global climate model projections and two emission scenarios, in annual climatic water deficit (DEF) and annual evapotranspiration (AET) by the 2080s relative to the historical reference period. Values represent relative changes in climate variable values in selected Douglas-fir (*Pseudotsuga menziesii*)-sampled cells in the Pacific Northwest states of Oregon and Washington. General cell locations and site elevations are provided along with historical and projected values for climate variables. Cells correspond to cells 1, 7, 19 and 20, respectively, in Fig. 5. See Appendix S1 for additional site information. Negative values indicate decreases relative to the historical reference period, and positive values represent increases. These sites were selected because they represent elevation and geographical ranges of the species sampled distribution (i.e. low to high elevation sites and north–south, east–west gradients).

Cell	Site elevation(s)	Climate variable	Climate model		
			PCM1_B1	COMP_A1B	HADGEM1_A1B
Quinault River, WA	440–960 m	Annual DEF (mm)	−26	−30	−12
		Annual AET (mm)	81	164	161
Dungeness Watershed, WA	803–1344 m	Annual DEF (mm)	22	76	118
		Annual AET (mm)	20	36	34
Stehekin, WA	444–1382 m	Annual DEF (mm)	38	139	164
		Annual AET (mm)	22	30	64
Bridge Creek North, WA	1027 m	Annual DEF (mm)	21	81	128
		Annual AET (mm)	31	57	71

increased AET of smaller magnitude and increasing DEF. Dry Cascade sites are projected to experience large DEF increases in the near absence of AET increases.

Energy- and water-limited Douglas-fir cells appear to be clustered, with energy-limited cells along a line of AET: DEF = 2:1 near the leftmost edge of climate space (Fig. 5a).

Although not easily delineated by geographical location or climate thresholds, trajectories through climate space differ for water-limited versus energy-limited cells. Most energy-limited cells display large AET and minor DEF increases throughout the 21st century (Fig. 5c). Some water-limited cells also display upward movement in climate space; these water-limited cells typically have higher AET:DEF than other water-limited cells for Douglas-fir. High AET:DEF suggests that water-limited cells in the Olympics could be considered less water-limited than water-limited cells in the Cascades. Conversely, more extremely water-limited cells for Douglas-

fir, especially in the eastern Olympics and drier northern Cascades, are projected to have increased DEF and minimal increased AET by 2080.

Based on examination of climatic conditions within selected cells to verify broader geographical patterns observed in climate space graphs (Tables 2–4), fine-scale patterns nearly always agreed with broad-scale patterns. For example, future SWE decreases were larger at higher elevations, and DEF was higher in eastern locations. We concluded that projections and climate–growth relationships were generally consistent throughout the study domain.

DISCUSSION

The methodology in this study is a simple yet effective way of assessing directional changes in radial tree growth at a broad scale in response to future climatic conditions. Label-
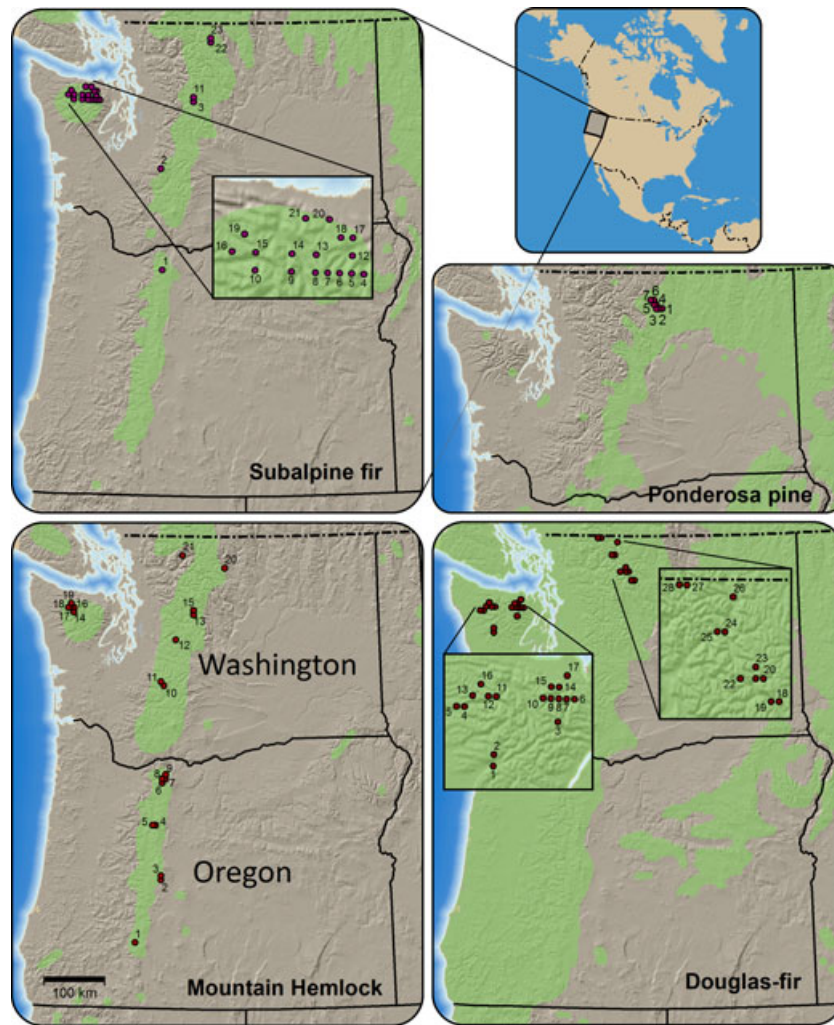
Figure 6 Species distribution for four coniferous species in Washington and Oregon. Shaded green areas represent species distributions, and points represent the location of Variable Infiltration Capacity (VIC) hydrological model cells that contain sampling sites from previous climate–growth studies. See Appendix S1 for a list of sampled site names and elevations within each cell.

ling sampled sites for each species as water- or energy-limited based on previously determined climate–growth relationships provided a means to categorize the predominant factors limiting growth. From here, we could make inferences about future growth, dependent on how climate projections suggest that limiting factors could change. Examining these changes across the species distribution and at selected sites reflecting the species elevational, geographical and climatic range, provides a basis for assessing future changes in productivity.

Changing growth environments across species distributions

Examining an entire species distribution in climate space, and observing how its distribution changes with time, allowed for general inferences regarding growth responses to climate change. These expected responses of individual spe-

cies are based on our understanding of climate–growth relationships and current limiting climatic factors. Mountain hemlock and subalpine fir environments will experience substantial decreases in future April 1 snow-water equivalent (SWE) and slight increases in summer climatic water deficit (DEF). Physiological responses in both species are expected to lead to increased radial growth. Higher temperature and lower SWE will lead to earlier snowmelt and higher soil temperature (Peterson & Peterson, 2001), facilitating earlier bud burst, shoot growth and stem growth (Worrall, 1983; Hansen-Bristow, 1986; Körner, 1998). Increased growing season length will lead to increased radial growth at sites where winter precipitation is currently dominated by snowpack. Longwave radiation and sky exposure can also affect growing season through their influence on frost (Jordan & Smith, 1995), and warmer temperatures that reduce frost frequency could increase the length and quality of the growing season. However, at some low elevation, dry sites, subalpine fir may

have minimal growth increases or decreased growth in response to an altered climate.

Douglas-fir and ponderosa pine growth environments will be characterized by large annual DEF increases relative to smaller actual evapotranspiration (AET) increases throughout the 21st century. These will increase moisture stress throughout most of these species distributions. Physiological responses to moisture stress – stomatal closure, reduced photosynthesis, and decreased carbon assimilation – will decrease growth (Kozlowski & Pallardy, 1997). When fewer carbohydrates are stored, cambial activity ultimately decreases (Lassoie, 1982). When water stress is high, available carbon is more likely to go first to root growth, increasing root absorption area (Waring, 1991) and limiting carbon availability for stem growth. Rapidly imposed water stress was shown to reduce net photosynthesis of Douglas-fir seedlings by 20–25% (Warren *et al.*, 2004), and under water-limited conditions, seedlings allocated more biomass to roots (Chan *et al.*, 2003), both of which would lead to decreased radial growth.

Interpreting spatial variations in species growth responses in climate space

Plotting the locations of sampled cells in climate space provided a basis to make inferences about spatial variation of growth responses within each species distribution. Assimilating geographical information, climate–growth relationship data, and observed cell trajectories helped determine expected growth responses at these sampled sites in the future. We can also make informed estimates of how unsampled cells in a similar area of climate space might respond to climatic change.

In climate space plots for mountain hemlock and subalpine fir, cells with higher initial SWE and lower DEF (left and upper edges of climate space) could experience large growth increases; these cells are often in the western Olympics and northern Cascades. Increased tree growth at some high elevation Cascade sites may be slightly offset by higher summer DEF in the Cascades compared to the Olympics (Table 2). These cells are found in the upper half of climate space, but farther to the right than most other cells in accordance with higher DEF (e.g. southern Cascades). In higher elevation cells, a larger decrease in SWE creates the potential for larger growth increases than at low elevation (Tables 2, 3). At some of the highest elevation subalpine fir sites in the Olympics (*c.*1800 m), snowmelt and bud burst do not occur until early summer, and growth ceases in late August (Ettl & Peterson, 1995). If April 1 snowpack is minimal as projected, growing season length could nearly double and greatly enhance growth. At lower elevation (*c.* 1300 m), growing season is a month longer than at high elevation, so growing season would not increase much and could even decrease as DEF increases.

Decreased mountain hemlock growth is possible in its southern range where summer DEF is consistently higher and future moisture stress is likely (Fig. 3). Trees represented by cells in the right-hand side of climate space already have water-limited tendencies (Peterson & Peterson, 2001). Although the strongest climate–growth relationship in southern Oregon is a negative correlation with snowpack depth (Peterson & Peterson, 2001), the presence of positive relationships with summer precipitation (absent in northern Washington) suggests that water is limiting. Therefore, tree growth in southern Oregon may not change or could decrease slightly if water availability decreases. Cells with increased DEF and decreased SWE (lower right portion of climate space) will be very likely to have lower growth, because water will be limiting in the absence of snowmelt.

Subalpine fir is also likely to experience lower growth in some locations, especially at currently water-limited sites in the eastern Olympics (bottom edge of climate space) (Fig. 4). At these sites, SWE is low relative to other locations, indicating that water deficit without sufficient moisture from snowmelt can result in a water-limited environment. In fact, these cells have lower SWE:DEF than all other cells. Projected DEF increases without increased soil moisture, as indicated by water-limited cell trajectories, could result in decreased growth. Photosynthesis in subalpine fir is reduced as much as 50% in an extreme drought year (Brodersen *et al.*, 2006), and if extreme droughts occur more often in the future, decreased subalpine fir growth is almost certain, especially where DEF is already high. In general, subalpine fir is more likely to have decreased growth than mountain hemlock because it is more common on drier sites in Washington and Oregon.

Sampled cells for Douglas-fir indicate that spatial variation in growth responses is likely to occur throughout its distribution. Decreased growth may be higher in cells that are historically severely water-limited, that is, cells with higher DEF: AET and PET:PPT (right-hand portions of climate space) (Fig. 5c), often including eastern Cascades sites. Cells for the Stehekin site are extreme examples of water-limitation where increased DEF could greatly decrease growth. Similarly, cells in the eastern Olympics are often co-located in climate space with eastern Cascade sites, indicating that areas in the Olympics may also have decreased growth. Climatic differences between the western and eastern Olympics demonstrate how future climate will in some cases vary over short distances, causing contrasting growth responses in Douglas-fir (Fig. 5).

The few energy-limited Douglas-fir cells are found at lower DEF (left and upper edges of climate space), areas of relatively high water supply and low evaporative demand. Trajectories of these cells move upward more than rightward, in contrast with most water-limited cells and are often located in the western Olympics (Fig. 5b,c). Elevated temperatures can increase Douglas-fir radial growth where soil moisture is adequate (Little *et al.*, 1995; Nigh *et al.*, 2004), so increased growth can be expected in energy-limited portions of climate space. Mildly water-limited cells in this same area could experience smaller increases in moisture stress and little change in growth. The few water-limited cells co-located

with energy-limited cells (upper-left portion of climate space) are less water-limited than most; DEF:AET is low relative to other water-limited cells in climate space. Projections of growth are consistent with recent data that document positive growth responses to higher daily temperatures at cool sites and negative growth responses at warm sites in the PNW (Williams *et al.*, 2010). Because energy-limited cells are located in the eastern and western Olympics as well as eastern and western Cascades, the geographical disparity makes energy-limited areas harder to pinpoint and growth responses by region more difficult to define, a function of the widespread distribution and tolerances of Douglas-fir. Although a distinct water- and energy-limitation classification was used to summarize climate–growth data, water and energy-limitation are categories that encompass a range of actual conditions.

Limitations of the climate space approach

Differences in scale between VIC output and tree species distribution maps can lead to overestimation of species distributions in climate space. Areas within a 25-km distribution grid cell may not have the species present, yet the VIC cell that coincides with that area is still included. Therefore, VIC cells outside the species distribution might be included in climate space plots, falsely representing climatic conditions for the species. The false addition of these VIC cells may make it appear that highlighted sampled cells do not demonstrate a thorough sampling of the species distribution, when in fact the species is not present in the 'unsampled' climate space. We examined this issue by determining which areas of Douglas-fir distribution reflect the majority (or highest density) of Douglas-fir occurrence relative to two different climate variables (Fig. 7). Vertical and horizontal lines associated with the *x*- and *y*-axes represent 10th and 90th percentiles of each climate variable where 10% or 90% of the species distribution is accounted for; violin plots represent the density of points for each variable. The resulting polygon encompasses the majority of Douglas-fir distribution in climate space while excluding locations where species occurrence is less common or perhaps inaccurately represented, providing a realistic extent of species range. Sites within the polygon provide a strong basis for understanding how the majority of a species distribution might respond to climate change, and sampled cells outside the polygons are distributional extremes where early responses to climate change might be detected.

In our methodology, climatic conditions are averaged across a VIC cell, and model projections are based on average cell elevation; therefore, local climatic conditions could be misrepresented if site elevation and average cell elevation differ. Sub-grid variation in local climate cannot always be captured at the scale of VIC output, leading to possible oversimplification of growth responses. Growth at individual sites within a cell can also be influenced by local factors such as root depth, soil and genetic variation.
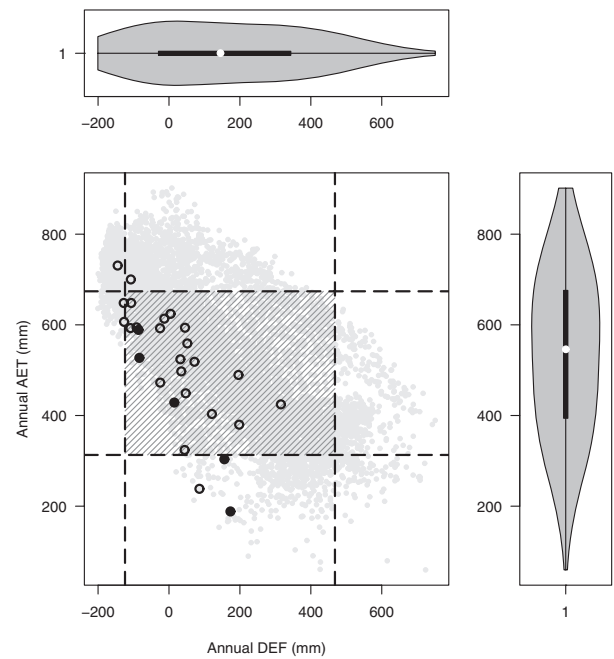
Figure 7 Douglas-fir (*Pseudotsuga menziesii*) distribution in climate space in the Pacific Northwest states of Oregon and Washington (open circles are water-limited cells and closed circles are energy limited). Percentile lines overlaid onto the graph represent the values of climatic water deficit (DEF) and actual evapotranspiration (AET) at which 10% and 90% of Douglas-fir distribution can be accounted for. Violin plots to the right and top of the graph represent the density of points in climate space relative to each climate variable.

Local knowledge is always needed to evaluate growth responses at a fine scale.

Shifts from energy- to water-limited forests in the PNW are likely, given projected changes in climate, and failure to consider potential shifts when interpreting growth responses to climate could lead to projected growth increases where decreases may actually occur. For example, higher growth is expected at most energy-limited subalpine fir and mountain hemlock sites, but changes in climate could induce shifts to water-limitation and cause decreased growth, especially at sites where SWE is already low. In climate space, this translates to cells initially having low SWE and high DEF, which could become moisture-stressed in a warmer climate. Cells projected to move into climate space that is currently water-limited are also good candidates for becoming more water-limited by the 2040s or 2080s and having lower tree growth. For energy-limited Douglas-fir sites, cells with low AET and high DEF are likely to become water-limited; these are sites with high DEF:AET that will increase in a warmer climate. Lower elevation and southern sites in each species range are where shifts in limiting climatic factors might occur first. Growth may not respond uniformly to climate variables over time, and plastic and adaptive behaviour in tree physiology will always affect estimates of growth response.

Using climate space to understand tree growth

We illustrated how growth responses of four tree species may vary across the landscape in response to climate change, based on data from previous climate–growth studies. Organizing this information in terms of climate space provides a visual means of projecting growth responses and extrapolating them beyond sampled areas. By examining where a geographical location falls in climate space relative to locations that have already been sampled and where climate–growth relationships are known, an expected growth response at a non-sampled location can be determined. This technique highlights areas within species distributions that may be more sensitive to climate change as defined by the extremity of the expected growth response or the potential for a shift in climatic factors that limit growth.

Expected growth responses in this study can help identify finer-scale responses for certain management activities. Identifying changes in tree growth can provide input for risk assessments of resources in a particular landscape, which are critical for developing strategies that facilitate adaptation to new climatic conditions (Vose *et al.*, 2012). Reduced radial growth can affect not only wood production, but can reduce tree vigour and resistance to stressors such as insects and fungal pathogens (Littell *et al.*, 2010). Cell trajectories in this study indicate where the biggest changes in climate may occur, portending changes in ecosystem function and suggesting priorities for monitoring. Species sensitivities may help guide decisions about where adaptation tactics could be focused (e.g. thinning water-limited Douglas-fir to reduce inter-tree competition and increase resilience to fire and insects). The appropriate management scale will depend on the scale of the ecological process of interest.

REFERENCES

Brodersen, C.R., Germino, M.J. & Smith, W.K. (2006) Photosynthesis during an episodic drought in *Abies lasiocarpa* and *Picea engelmannii* across an alpine treeline. *Arctic, Antarctic, and Alpine Research*, **38**, 34–41.

Case, M.J. & Peterson, D.L. (2005) Fine-scale variability in growth–climate relationships of Douglas-fir, North Cascade Range, Washington. *Canadian Journal of Forest Research*, **35**, 2743–2755.

Chan, S.S., Radosevich, S.R. & Grotta, A.T. (2003) Effects of contrasting light and soil moisture availability on the growth and biomass allocation of Douglas-fir and red alder. *Canadian Journal of Forest Research*, **33**, 106–117.

Chen, P.Y., Welsh, C. & Hamann, A. (2010) Geographic variation in growth response of Douglas-fir to interannual climate variability and projected climate change. *Global Change Biology*, **16**, 3374–3385.

Climate Impacts Group (2010) *Columbia Basin Climate Change Scenarios Project*. University of Washington. Available at: http://warm.atmos.washington.edu/2860/.

Cook, E.R. & Kairiukstis, L.A. (eds) (1990) *Methods of dendrochronology: applications in the environmental sciences*. Kluwer Academic Publishers, Dordrecht.

Elsner, M.M., Cuo, L., Voisin, N., Deems, J.S., Hamlet, A.F., Vano, J.A., Mickelson, K.E.B., Lee, S. & Lettenmaier, D.P. (2010) Implications of 21st century climate change for the hydrology of Washington State. *Climatic Change*, **102**, 225–260.

Ettl, G.J. & Peterson, D.L. (1995) Growth response of subalpine fir (*Abies lasiocarpa*) to climate in the Olympic Mountains, Washington, USA. *Global Change Biology*, **1**, 213–230.

Fagre, D.B., Peterson, D.L. & Hessl, A.E. (2003) Taking the pulse of mountains: ecosystem responses to climatic variability. *Climatic Change*, **59**, 263–282.

Franklin, J.F. & Dyrness, C.T. (1988) *Natural vegetation of Oregon and Washington*. Oregon State University Press, Corvallis, OR.

Fritts, H.C. (1976) *Tree rings and climate*. Academic Press, London.

Gedalof, Z. & Smith, D.J. (2001) Dendroclimatic response of mountain hemlock (*Tsuga mertensiana*) in Pacific North America. *Canadian Journal of Forest Research*, **31**, 322–332.

Hamlet, A. F., Carrasco, P., Deems, J., Elsner, M. M., Kamstra, T., Lee, C., Lee, S-Y., Mauger, G., Salathé, E. P., Tohver, I. & Whitely Binder, L. (2010) *Final project report for the Columbia Basin Climate Change Scenarios Project*. Available at: http://warm.atmos.washington.edu/2860/report/.

Hansen-Bristow, K.J. (1986) Influence of increasing elevation on growth characteristics at timberline. *Canadian Journal of Botany*, **64**, 2517–2523.

Henderson, J. A., Peter, D. H., Lesher, R. D. & Shaw, D. C. (1989) *Forested plant associations of the Olympic National Forest*. USDA Forest Service Pacific Northwest Region, Ecological Technical Paper, 001-88, Olympia, WA.

Holman, M.L. & Peterson, D.L. (2006) Spatial and temporal variability in forest growth in the Olympic Mountains, Washington: sensitivity to climatic variability. *Canadian Journal of Forest Research*, **36**, 92–104.

Huang, J., Tardif, J.C., Bergeron, Y., Denneler, B., Berninger, F. & Girardin, M.P. (2010) Radial growth response of four dominant boreal tree species to climate along a latitudinal

gradient in the eastern Canadian boreal forest. *Global Change Biology*, **16**, 711–731.

Jordan, D.N. & Smith, W.K. (1995) Microclimate factors influencing the frequency and duration of growth season frost for subalpine plants. *Agricultural and Forest Meteorology*, **77**, 17–30.

Knutson, K.C. & Pyke, D.A. (2008) Western juniper and ponderosa pine ecotonal climate–growth relationships across landscape gradients in southern Oregon. *Canadian Journal of Forest Research*, **38**, 3021–3032.

Körner, C. (1998) A re-assessment of high elevation treeline positions and their explanation. *Oecologia*, **115**, 445–459.

Kozlowski, T.T. & Pallardy, S.G. (1997) *Physiology of woody plants*, 2nd edn. Academic Press, San Diego, CA.

Kusnierczyk, E.R. & Ettl, G.J. (2002) Growth response of ponderosa pine (*Pinus ponderosa*) to climate in the eastern Cascade Mountains, Washington, U.S.A.: implications for climatic change. *Ecoscience*, **9**, 544–551.

Laroque, C.P. & Smith, D.J. (2003) Radial growth forecasts for five high-elevation conifer species on Vancouver Island, British Columbia. *Forest Ecology and Management*, **183**(1–3), 313–325.

Lassoie, J. P. (1982) Physiological activity in Douglas-fir. *Analysis of coniferous forest ecosystems in the Western United States* (ed. by R.L. Edmonds), pp. 126–185. Hutchison Ross Publishing Company, Stroudsberg, PA.

Liang, X., Lettenmaier, D. P., Wood, E. F. & Burges, S. J. (1994) A simple hydrologically based model of land surface water and energy fluxes for general circulation models. *Journal of Geophysical Research*, **99**, 14,415–14,428.

Littell, J.S., Peterson, D.L. & Tjoelker, M. (2008) Douglas-fir growth in mountain ecosystems: water limits tree growth from stand to region. *Ecological Monographs*, **78**, 349–368.

Littell, J.S., Oneil, E.E., McKenzie, D., Hicke, J.A., Lutz, J.A., Norheim, R.A. & Elsner, M.M. (2010) Forest ecosystems, disturbance, and climatic change in Washington State, USA. *Climatic Change*, **102**, 129–158.

Little, E. L., Jr (1971) *Atlas of United States trees, Vol. 1: Conifers and important hardwoods*. US Department of Agriculture Miscellaneous Publication 1146, Washington, DC.

Little, R.L., Peterson, D.L., Silsbee, D.G., Shainsky, L.J. & Bednar, L.F. (1995) Radial growth patterns and the effects of climate on second growth Douglas-fir (*Pseudotsuga menziesii*) in the Siskiyou Mountains, Oregon. *Canadian Journal of Forest Research*, **25**, 724–735.

Lookingbill, T.R. & Urban, D.L. (2005) Gradient analysis, the next generation: towards more plant-relevant explanatory variables. *Canadian Journal of Forest Research*, **35**, 1744–1753.

Mantua, N.J., Hare, S.R., Zhang, Y., Wallace, J.M. & Francis, R.C. (1997) A Pacific interdecadal climate oscillation with impacts on salmon production. *Bulletin of the American Meteorological Society*, **78**, 1069–1079.

Miles, E.L., Elsner, M.M., Littell, J.S., Binder, L.W. & Lettenmaier, D.P. (2010) Assessing regional impacts and adaptation strategies for climate change: the Washington

climate change impacts assessment. *Climatic Change*, **102**, 9–27.

Mote, P.W. & Salathé, E.P. (2010) Future climate in the Pacific Northwest. *Climatic Change*, **102**, 29–50.

Nakawatase, J.M. & Peterson, D.L. (2006) Spatial variability in forest growth–climate relationships in the Olympic Mountains, Washington. *Canadian Journal of Forest Research*, **36**, 77–91.

Nakićenović, N. & Swart, R. (eds) (2000) *Special report on emissions scenarios: a special report of Working Group III of the Intergovernmental Panel on Climate Change*. Cambridge University Press, Cambridge.

Nigh, G.D., Ying, C.C. & Qian, H. (2004) Climate and productivity of major conifer species in the interior of British Columbia, Canada. *Forest Science*, **50**, 659–671.

Nijssen, B.N., Lettenmaier, D.P., Liang, X., Wetzel, S.W. & Wood, E.F. (1997) Streamflow simulation for continental-scale river basins. *Water Resources Research*, **33**, 711–724.

Peterson, D. L. (1998) Climate, limiting factors and environmental change in high-altitude forests of western North America. *Climatic variability and extremes: the impact on forests* (ed. by M. Beniston and J.L. Innes), pp. 191–208. Springer-Verlag, Heidelberg.

Peterson, D.W. & Peterson, D.L. (1994) Effects of climate on radial growth of sub-alpine conifers in the North Cascade Mountains. *Canadian Journal of Forest Research*, **24**, 1921–1932.

Peterson, D.W. & Peterson, D.L. (2001) Mountain hemlock growth responds to climatic variability at annual and decadal time scales. *Ecology*, **82**, 3330–3345.

Peterson, D.L., Schreiner, E.G. & Buckingham, N.M. (1997) Gradients, vegetation, and climate: spatial and temporal dynamics in the Olympic Mountains, USA. *Global Ecology and Biogeography Letters*, **6**, 7–17.

Peterson, D.W., Peterson, D.L. & Ettl, G.J. (2002) Growth responses of subalpine fir to climatic variability in the Pacific Northwest. *Canadian Journal of Forest Research*, **32**, 1503–1517.

R Development Core Team (2009) *R: a language and environment for statistical computing*. R Foundation for Statistical Computing, Vienna, Austria. Available at: http://www.R-project.org.

Randall, D. A., Wood, R. A., Bony, S., Colman, R., Fichefet, T., Fyfe, J., Kattsov, V., Pitman, A., Shukla, J., Srinivasan, J., Stouffer, R. J., Sumi, A. & Taylor, K. E. (2007) Climate models and their evaluation. *Climate change 2007: the physical science basis. Contribution of Working Group I to the Fourth Assessment Report of the Intergovernmental Panel on Climate Change* (ed. by S. Solomon, D. Qin, M. Manning, Z. Chen, M. Marquis, K.B. Averyt, M. Tignor and H.L. Miller) Cambridge University Press, Cambridge.

Shinker, J.J. & Bartlein, P.J. (2010) Spatial variations of effective moisture in the western United States. *Geophysical Research Letters*, **37**, L02701.

Stephenson, N.L. (1990) Climatic control of vegetation distribution – the role of the water balance. *The American Naturalist*, **135**, 649–670.

Stephenson, N.L. (1998) Actual evapotranspiration and deficit: biologically meaningful correlates of vegetation distribution across spatial scales. *Journal of Biogeography*, **25**, 855–870.

Vose, J., Peterson, D.L. & Patel-Weynand, T. (2012) *Effects of climatic variability and change on forest ecosystems: a comprehenszrive science synthesis for the U.S. forest sector*. USDA Forest Service General Technical Report PNW-GTR-870. Pacific Northwest Research Station, Portland, OR.

Waring, R. H. (1991) Responses of evergreen trees to multiple stresses. *Response of plants to multiple stresses* (ed. by H.A. Mooney, W.E. Winner and E.J. Pell), pp. 371–390. Academic Press, San Diego, CA.

Warren, C.R., Livingston, N.J. & Turpin, D.H. (2004) Water stress decreases the transfer conductance of Douglas-fir (*Pseudotsuga menziesii*) seedlings. *Tree Physiology*, **24**, 971–979.

Williams, A.P., Michaelsen, J., Leavitt, S.W. & Still, C.J. (2010) Using tree rings to predict the response of tree growth to climate change in the continental United States during the twenty-first century. *Earth Interactions*, **14**, 1–20.

Worrall, J. (1983) Temperature–bud-burst relationships in amabilis and subalpine fir provenance tests replicated at different elevations. *Silvae Genetica*, **32**, 203–209.

SUPPORTING INFORMATION

Additional Supporting Information may be found in the online version of this article:

Appendix S1 Species sampling site and climate–growth relationship information.

BIOSKETCHES

Whitney L. Albright is a climate change associate working in cooperation with the Climate Science Program at the California Department of Fish and Wildlife where she helps integrate climate change into management and planning efforts for fish, wildlife, and habitats in California. She has conducted research on climate change in mountain ecosystems of the Pacific Northwest region of the United States, and is interested in evaluating the impacts and implications of climate change to natural resource management.

David L. Peterson is a research biologist at the U.S. Forest Service, Pacific Northwest Research Station in Seattle where he is team leader for the Fire and Environmental Research Applications team. He has conducted research on fire ecology and climate change in mountain ecosystems throughout the western United States, and has published over 200 scientific articles and three books. He is a principal investigator for the Western Mountain Initiative and a contributing author for the Intergovernmental Panel on Climate Change and the U.S. National Climate Assessment.

Editor: Peter Linder